



# Tropospheric mercury vertical profiles between 500 and 10 000 m in central Europe

Andreas Weigelt<sup>1,a</sup>, Ralf Ebinghaus<sup>1</sup>, Nicola Pirrone<sup>2</sup>, Johannes Bieser<sup>1,3</sup>, Jan Bödewadt<sup>1</sup>, Giulio Esposito<sup>2</sup>, Franz Slemr<sup>4</sup>, Peter F. J. van Velthoven<sup>5</sup>, Andreas Zahn<sup>6</sup>, and Helmut Ziereis<sup>3</sup>

<sup>1</sup>Helmholtz-Zentrum Geesthacht (HZG), Institute of Coastal Research, Geesthacht, Germany

<sup>2</sup>National Research Council (CNR), Institute of Atmospheric Pollution Research, Rende, Italy

<sup>3</sup>Deutsches Zentrum für Luft- und Raumfahrt (DLR), Institute of Atmospheric Physics, Oberpfaffenhofen, Germany

<sup>4</sup>Max-Planck-Institute for Chemistry (MPI-C), Department of Atmospheric Chemistry, Mainz, Germany

<sup>5</sup>Royal Netherlands Meteorological Institute (KNMI), Chemistry and Climate Division, De Bilt, the Netherlands

<sup>6</sup>Karlsruhe Institute of Technology (KIT), Institute of Meteorology and Climate Research, Karlsruhe, Germany

<sup>a</sup>now at Federal Maritime and Hydrographic Agency (BSH), Hamburg, Germany

Correspondence to: Andreas Weigelt (andreas.weigelt@bsh.de) and Ralf Ebinghaus (ralf.ebinghaus@hzg.de)

Received: 18 July 2015 – Published in Atmos. Chem. Phys. Discuss.: 20 October 2015

Revised: 19 February 2016 – Accepted: 16 March 2016 – Published: 30 March 2016

**Abstract.** The knowledge of the vertical distribution of atmospheric mercury (Hg) plays an important role in determining the transport and cycling of mercury. However, measurements of the vertical distribution are rare, because airborne measurements are expensive and labour intensive. Consequently, only a few vertical Hg profile measurements have been reported since the 1970s. Besides the Civil Aircraft for the Regular Investigation of the atmosphere Based on an Instrument Container (CARIBIC) observations, the latest vertical profile over Europe was measured in 1996. Within the Global Mercury Observation System (GMOS) project, four vertical profiles were taken on board research aircraft (CASA-212) in August 2013 in background air over different locations in Slovenia and Germany. Each vertical profile consists of at least seven 5 min horizontal flight sections from 500 m above ground to 3000 m a.s.l. Gaseous elemental mercury (GEM) and total gaseous mercury (TGM) were measured with Tekran 2537X and Tekran 2537B analysers. In addition to the mercury measurements, SO<sub>2</sub>, CO, O<sub>3</sub>, NO, and NO<sub>2</sub>, basic meteorological parameters (pressure, temperature, relative humidity) have been measured. Additional ground-based mercury measurements at the GMOS master site in Waldhof, Germany and measurements onboard the CARIBIC passenger aircraft were used to extend the profile to the ground and upper troposphere respectively.

No vertical gradient was found inside the well-mixed boundary layer (variation of less than 0.1 ng m<sup>-3</sup>) at different sites, with GEM varying from location to location between 1.4 and 1.6 ng m<sup>-3</sup> (standard temperature and pressure, STP:  $T = 273.15$  K,  $p = 1013.25$  hPa). At all locations GEM dropped to 1.3 ng m<sup>-3</sup> (STP) when entering the free troposphere and remained constant at higher altitudes. The combination of the vertical profile, measured on 21 August 2013 over Leipzig, Germany, with the CARIBIC measurements during ascent and descent to Frankfurt Airport, Germany, taken at approximately the same time, provide a unique central European vertical profile from inside the boundary layer (550 m a.s.l.) to the upper free troposphere (10 500 m a.s.l.) and show a fairly constant free-tropospheric TGM concentration of 1.3 ng m<sup>-3</sup> (STP).

## 1 Introduction

Mercury and its compounds are very toxic and therefore, hazardous for human health and the environment (Selin, 2009). Consequently, mercury is on the priority list of many international agreements and conventions dealing with environmental protection and human health, including the United Nations Environment Programme (UNEP) Minamata Convention on Mercury (www.mercuryconvention.org). Mercury is

**Table 1.** Summary of all known European airborne atmospheric mercury measurements until December 2014.

Time	Location	Altitude	Key finding	Literature
1978–1981	Central Europe	6–12 km	– no vertical gradient	Slemr et al. (1985)
1981	West of Göteborg	up to 3 km	– decrease with altitude proportional to pressure decrease → no vertical gradient when transferring to STP conditions	Brosset (1987)
June 1988	Eastern Lithuania	not given	– concentration proportional to pressure at sampling altitude → no vertical gradient when transferring to STP conditions	Kvietkus (1995)
June 1996	Eastern Germany	0.5–3.75 km	– no vertical gradient – increased concentration observed near source region up to ~ 2 km altitude	Ebinghaus and Slemr (2000)
since 2005	Europe and global (CARIBIC Project)	6–12 km	– long term monitoring in UT and LS (trend analysis) – large-scale plume identification	Slemr et al. (2009, 2014) www.caribic-atmospheric.com
July/August 2012	Mt Etna volcano (Southern Italy)	0–4 km	– no/low gaseous mercury emission from Mt Etna volcano	www.gmos.eu
August 2013	Central Europe (Slovenia and Germany)	0–3 km 6–11 km	– significant difference between boundary layer and free troposphere, but no vertical gradient inside individual layers	this study

emitted to the atmosphere from a variety of anthropogenic (e.g. coal and oil combustion) and natural sources (e.g. evaporation from ocean and lakes) (Pirrone et al., 2010). The most efficient transport pathway for mercury is the atmosphere (Fitzgerald et al., 1998). However, measurements of the vertical distribution of atmospheric mercury are rare, because airborne measurements are time consuming and expensive. Between 1978 and 2015 only seven campaigns performed airborne mercury measurements over Europe. Apart from the CARIBIC measurements (Civil Aircraft for the Regular Investigation of the atmosphere Based on an Instrument Container, www.caribic-atmospheric.com) in the upper troposphere, the last European vertical profile of mercury was measured in June 1996. Table 1 summarizes all European airborne mercury measurements known to us, together with their key findings (including this study).

The GMOS (Global Mercury Observation System; www.gmos.eu) 2012 measurement campaign at Mt Etna focused on volcanic emissions and no vertical profile was measured. CARIBIC measurements focus on the tropopause region and determine vertical profiles only above 6 km during ascent and descent from and to airports. During the four measurement campaigns over Europe between 1978 and 1996, a vertical gradient was found neither in the planetary boundary layer (PBL) nor in the free troposphere. This was expected, because most of the atmospheric mercury is in its elemental

state Hg(0) with a long atmospheric lifetime of six months to one year (Lindberg et al., 2007). Due to the long lifetime, Hg is well mixed in the atmosphere. All vertical profile measurements of Hg until 2009 were summarized by Swartzendruber et al. (2009) (data are shown in Fig. 7 for comparison to this study). Hg vertical profiles were measured by Radke et al. (2007), Talbot et al. (2008), and Swartzendruber et al. (2006, 2008) in different locations over the Pacific Ocean and the US between 2002 and 2008. Vertical profiles over Canada were reported by Banic et al. (2003) for the period between 1995 and 1998. Friedli et al. (2004) report vertical profiles measured over Japan/Korea and China in spring 2001. In the Swartzendruber et al. (2009) summary, a paper by Ebinghaus and Slemr (2000) represents the only European vertical profile. Brooks et al. (2014) reported speciated mercury vertical profiles measured over the US over a period of almost one year from August 2012 to June 2013. Recently, Shah et al. (2016) published total Hg (THg) and oxidized Hg (Hg(II)) vertical profiles measured over the south-eastern US between 1 June and 15 July 2013. The August measurement from Brooks et al. (2014) and the averaged data from Shah et al. (2016) are shown in Fig. 7 as well.

Except for large vertical GEM (gaseous elemental mercury) gradients reported by Radke et al. (2007) and in April, May, and June by Brooks et al. (2014), no pronounced GEM vertical gradients were observed by other researchers in other



**Figure 1.** Flight tracks of the European Tropospheric Mercury Experiment part 2 (ETMEP-2) research flights in August 2013. Flights are separated by the flight track colour. The home base of the used aircraft was Parma, Italy. Vertical profiles were flown over Iskraba and Idrija (Slovenia), and Lippendorf, Leipzig, and Waldhof (Germany)

months (Swartzendruber et al., 2009; Brooks et al., 2014; Shah et al., 2016). Usually the GEM concentrations in the planetary boundary layer (PBL; ground to 1–3 km) were found to be similar to those in the lower free troposphere (FT). As mercury is emitted by sources on the ground, we would expect at least a slightly higher concentration inside the PBL compared to the FT. The absence of a vertical gradient inside the PBL and the FT is caused by the “fast” mixing velocity of Hg (hours to days), compared to the atmospheric lifetime (6 to 12 month) and the insufficient precision of the available mercury analysers to detect concentration gradients of less than  $0.1 \text{ ng m}^{-3}$ .

The European Tropospheric Mercury Experiment (ETMEP) was carried out in July/August 2012 (ETMEP-1) and August 2013 (ETMEP-2) to measure local emissions and to perform vertical profile measurements from inside the boundary layer to the lower free troposphere. In total 10 measurement flights were performed over Italy, Slovenia, and Germany with two small, flexible aircraft. The ETMEP-1 campaign focused on volcanic emissions and not on the

investigation of vertical profiles. We report here the results of the ETMEP-2 campaign, which focused on vertical profile measurements over central Europe.

## 2 Measurement location and methodology

From 19 to 22 August 2013, five ETMEP-2 measurement flights were carried out over central Europe (Fig. 1). After take off on 19 August at the aircraft’s home base in Parma, northern Italy, the first vertical profile was measured in the early afternoon over the GMOS master site in Iskraba, Slovenia. Thereafter the second vertical profile was flown over Idrija, a former mercury mining area in Slovenia. On the morning of 21 August, the transfer flight from Ronchi dei Legionari in the north-eastern Italy to Leipzig in central Germany, was used as the second measurement flight to obtain a central European horizontal profile inside or slightly above the boundary layer (flight 2). During this flight no vertical profile was flown. After refuelling at Leipzig/Halle Airport, the third flight was carried out on the same day. Within this flight, two vertical profiles were flown; the first one at noon downwind of a coal-fired power plant south of Leipzig (Lippendorf) and the second one in the early afternoon over Leipzig city centre. With the fourth measurement flight on 22 August (take off from Leipzig/Halle Airport), the fifth vertical profile was flown in the late morning over the GMOS master site in Waldhof, northern Germany, representing central European rural background air. Thereafter, the aircraft was refuelled at Leipzig/Halle Airport and flown back to Parma on the same day. This last transfer flight (flight 5) was used to obtain a second central European horizontal profile slightly above the boundary layer. Here we present and discuss the vertical profiles over Iskraba, Idrija, Leipzig, and Waldhof. The vertical profile downwind of the Lippendorf coal-fired power plant will be discussed in a separate paper (Weigelt et al., 2016).

Each vertical profile consists of at least seven horizontal flight legs, lasting 5 min each. The altitude for the flight legs was chosen, starting inside the boundary layer at about 400 m above ground. For each vertical profile the highest flight level was 3000 m a.s.l. (metres above sea level). Each flight level change was performed within 2.5 min. Consequently, each vertical profile took 50 min, being representative of the transitory situation at a certain measurement location. The campaign was performed with a CASA 212 two engine turboprop aircraft (Fig. 2a) operated by Compagnia Generale Ripresearee (<http://www.terraitaly.it>). The CASA 212 has a maximum payload of 2.7 tons, allowing it to carry the measurement instruments, various service instruments, the power supply, two pilots, and five operators. The aircraft normal cruising speed is 140 kn ( $\sim 260 \text{ km h}^{-1}$ ). At this speed the maximum flight distance is  $\sim 1600 \text{ km}$ . The maximum flight level of the unpressurized aircraft is 8500 m. As it was not possible to fly with oxygen masks, the maximum flight

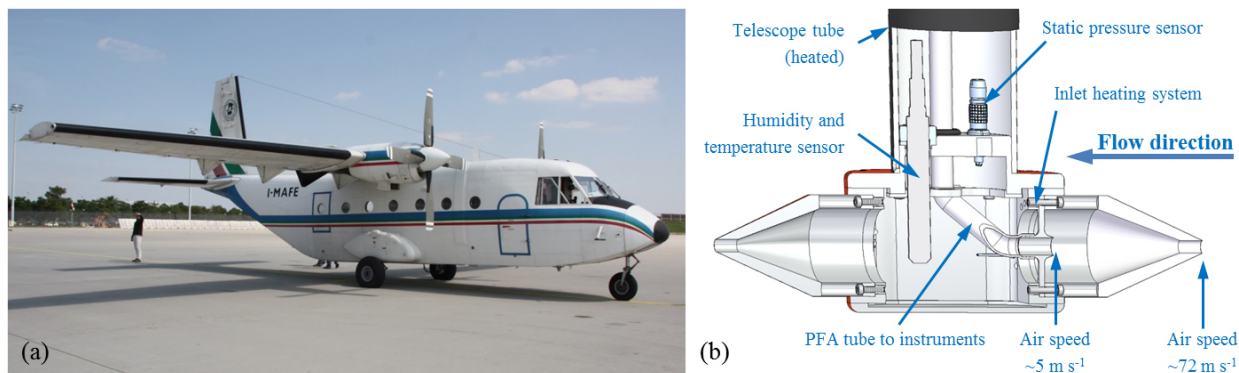


**Figure 2.** For the ETMEP-2 campaign in August 2013 the CASA 212 (a) from the Italian company Compagnia Generale Ripresearee (<http://www.terraitaly.it/>) was equipped with a specially designed and manufactured PTFE-coated trace gas inlet (b).

level for the ETMEP-2 campaign was limited to 10 000 ft ( $\sim 3000$  m a.s.l.).

Previously, the CASA 212 was used as a research aircraft to carry remote sensing LIDAR (light detection and ranging) systems, but not for in situ measurements. Therefore, the aircraft had no gas inlet. To transfer unbiased ambient air from outside the aircraft boundary layer to the measurement instruments, a gas inlet system has been developed and manufactured at the Helmholtz-Zentrum Geesthacht (Fig. 2b). The gas inlet was designed specifically for the cruising speed of the CASA 212. The air enters the inlet with a speed of about  $260 \text{ km h}^{-1}$  ( $\sim 72 \text{ m s}^{-1}$ ). By expansion, the air velocity is reduced to about  $15 \text{ km h}^{-1}$  ( $\sim 5 \text{ m s}^{-1}$ ). At  $260 \text{ km h}^{-1}$  about  $120 \text{ L min}^{-1}$  (ambient conditions) enters the inlet. In the centre of the expansion area the main sampling line starts, taking only the core flow without contact with the inlet surface. All instruments pull their sample air from this main sampling line (all together about  $25 \text{ L min}^{-1}$ ). The remaining  $95 \text{ L min}^{-1}$  are directed to the back of the inlet where the air speed is increased by a nozzle and the air exits. By replacing the inlet and outlet nozzles with smaller or larger ones, this inlet system can be adapted for other aircraft types with different cruising speeds. In the expanded area (behind the main sample line) the air temperature ( $T$ ), static pressure ( $p$ ), and relative humidity (RH) are measured. To optimize for trace gas measurements and to avoid contamination, the whole inside of the inlet was coated with PTFE (polytetrafluoroethylene) and only PFA (perfluoroalkoxy alkane) tubes were used for the sampling line. The outside of the inlet was copper coated to avoid electrostatic charging. The inlet body was mounted onto a 6 cm wide and 90 cm long telescope tube. This telescope tube was flexibly mounted into the aircraft fuselage. After take off, the telescope tube was pushed down by  $\sim 40$  cm from inside the aircraft to ensure the inlet nozzle was outside the aircraft boundary layer. Before landing, the telescope tube was pulled back into the aircraft fuselage. The inlet and telescope tube were equipped with controllable heaters to prevent icing. However, because

the measurement flights were carried out in summer at altitudes below 3000 m a.s.l., it was never necessary to switch on the heating system. Inside the cabin the tubing from the telescope tube to the instruments ( $\sim 2.5$  m long  $3/8''$  main sample tube with PFA manifolds to instruments; residence time  $< 0.3$  s) was not heated. The temperature inside the cabin was 18 to  $30^\circ\text{C}$ . Aerosol particles were filtered out at the instrument's individual inlets using a PTFE membrane filter (pore size  $0.2 \mu\text{m}$ ). All data were synchronized using individual instrument lag and response time.

For the campaign, the aircraft was equipped with two mercury measurement instruments, a Tekran 2537B and a Tekran 2537X (cf. Table 2). Both analysers are based on cold vapour atomic fluorescence spectroscopy (CVAFS) and can measure total gaseous mercury (TGM; Slemr et al., 2016). Because the CVAFS needs pre-concentrated samples, the Tekran analysers pre-amalgamate Hg from the sample air on solid gold cartridges and achieve a minimum temporal resolution of 150 s. For the ETMEP-2 flights a quartz wool trap was installed upstream the Tekran 2537X analyser, removing only gaseous oxidized mercury (GOM) and aerosol particles with particle bound mercury (PBM) but no GEM from the air stream (cf. Lyman and Jaffe, 2011).

The Tekran 2537B analyser was operated as backup instrument without a quartz wool trap. The PFA- and PTFE-made gas inlet and tubing system were not tested for GOM transmission efficiency. However, the residence time of the sampled air in the PFA tubing connecting the inlet and the instruments is shorter than 0.3 s. An international field inter-comparison (Ebinghaus et al., 1999) has concluded that under such conditions, mercury measurements represent TGM ( $\text{TGM} = \text{GEM} + \text{GOM}$ ). The capture of GOM by the gold traps and its conversion to GEM during the thermal desorption is discussed by Slemr et al. (2016). Consequently, we believe our Tekran 2537B measurements approximate TGM concentrations with an uncertainty of 12.5%. The uncertainty has been calculated by Weigelt et al. (2013) using two different approaches according to ISO 20988

**Table 2.** List of instruments installed into the CASA 212 research aircraft. The acronyms are defined as GEM (gaseous elemental mercury), GOM (gaseous oxidized mercury), CO (carbon monoxide), O<sub>3</sub> (ozone); SO<sub>2</sub> (sulphur dioxide); NO (nitric oxide); NO<sub>2</sub> (nitric dioxide).

Parameter	Instrument name	Temporal resolution	Uncertainty	Lower detection limit
GEM	Tekran: 2537X (with upstream quartz wool trap)	150 s	±12.5 % of reading	0.1 ng m <sup>-3</sup>
GEM + unknown amount of GOM <sup>a</sup>	Tekran 2537B	150 s	±12.5 % of reading	0.1 ng m <sup>-3</sup>
CO	Aero Laser AL5002	1 s	±3 % of reading	1.5 ppb
O <sub>3</sub>	Teledyne API 400A	10 s	±2 % of reading	0.6 ppb
SO <sub>2</sub>	Thermo: 43C Trace Level	10 s	±4 % of reading	0.2 ppb
NO, NO <sub>2</sub>	Teledyne API M200EU	10 s	±10 % of reading	0.05 ppb
Pressure	Sensor Technics CTE7001	1 s	±1 % of reading	0 mbar
Temperature	LKM Electronic DTM5080	1 s	±0.13 °C	-50 °C
Relative Humidity (RH)	Vaisala HMT333	8 s	±1.0 % RH (0–90 % RH) ±1.7 % RH (90–100 % RH)	0 %
GPS data (3rd position, speed, heading)	POS AV	1 s	±5 m (horizontal) <sup>b</sup> ±15 m (vertical) <sup>b</sup>	–

<sup>a</sup> The aircraft inlet system transmission efficiency for GOM was not tested.

<sup>b</sup> The GPS accuracy is dependent on the number of satellites. The given numbers are estimated values.

type A6 and ISO 20988 Type A2. This uncertainty complies with the quality objective of the EU air quality directive 2004/107/EC. The instrumental set-up in the aircraft was almost identical and therefore, we expect the uncertainty to be very similar. Calculating GOM concentrations from the TGM and GEM difference (Temme et al., 2003a; Slemr et al., 2009; Lyman and Jaffe, 2011) is limited by its uncertainty ( $\sim 150 \text{ pg m}^{-3}$ ), which is larger than the expected GOM concentrations (few tens of  $\text{pg m}^{-3}$ ). Therefore, GOM concentrations are not presented.

For the identification and characterization of different air masses carbon monoxide (CO), ozone (O<sub>3</sub>), sulphur dioxide (SO<sub>2</sub>), nitric oxide (NO), nitric dioxide (NO<sub>2</sub>), and the basic meteorological parameters: temperature ( $T$ ), pressure ( $p$ ), and relative humidity (RH), were measured simultaneously at high temporal resolution (cf. Table 2). Uncertainties of these parameters were calculated according to the individual instrument uncertainty given by the manufacturer and the calibration gas accuracy (CO, O<sub>3</sub>, SO<sub>2</sub>, NO) and are summarized together with instrument details in Table 2. CO and SO<sub>2</sub> can be used for the identification of city plumes and plumes of power stations respectively (Parrish et al., 1991; Klemp et al., 2002; Jaffe et al., 2005; Slemr et al., 2014). O<sub>3</sub> can be used to characterize upper tropospheric/lower stratospheric air or to explain oxidation processes (Zahn and Brenninkmeijer, 2003). An increased NO<sub>x</sub> (NO + NO<sub>2</sub>) mixing ratio can indicate combustion plumes (Ambrose et al., 2015; Weigelt et al., 2016) too. Usually FT air is drier than PBL air (Spencer and Braswell, 1996) and therefore, the RH measurements

can distinguish these two air masses. For additional information, model meteorological data, e.g. potential vorticity, equivalent potential temperature, relative and specific humidity, cloud cover, cloud water content, 3-dimensional wind vector, as well as 5-day backward and 2-day forward trajectories have been calculated every 150 s along the aircraft flight tracks according to the CARIBIC scheme ([http://www.knmi.nl/samenw/campaign\\_support/CARIBIC/](http://www.knmi.nl/samenw/campaign_support/CARIBIC/)). These calculations are based on meteorological analysis data from the European Centre for Medium-Range Weather Forecasts (ECMWF) and the TRAJKS trajectory model (Scheele et al., 1996).

Before take off, all instruments were warmed up for at least 45 min, using an external ground power supply. During the starting of the engines, the power was interrupted for less than 3 min. Since 45 min were too short to stabilize the Tekran 2537 internal permeation source, these instruments were calibrated directly after each measurement flight before the engine shut down. All data were recalculated, using the post-flight calibration. The pressure in the fluorescent cells of both Tekran instruments was kept constant using upstream pressure controllers at the exits of the cells. This eliminated the known pressure dependence of the response signal (Ebinghaus and Slemr, 2000; Talbot et al., 2007). During profiling, the temperature in the cabin was relatively constant. Sampling flow rate responds to changing altitude within a few seconds and flow rate fluctuations are accounted for by the integration of flow rate over the sampling interval. The CO instrument calibration takes 60 s and therefore, was performed during the measurement flights every 20 min. The

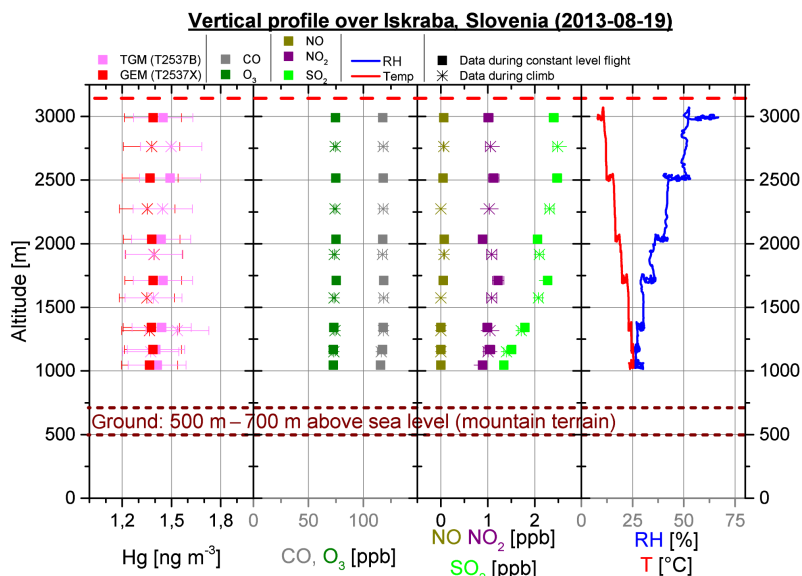


**Figure 3.** Vertical profile measured on 19 August 2013 from 13:17:30 to 14:07:30 (local time) over the GMOS master site Iskraba (45.561° N, 14.858° E, elevation: 530 m a.s.l.; mountain terrain). Squares represent 300 s averages with horizontal flight leg; stars indicate 150 s averages during climbing between two neighbouring flight legs. The red dashed line indicates the planetary boundary layer (PBL) top, which is not representative here because all measurements were performed below the boundary layer top. GEM and TGM concentrations are given at standard temperature and pressure ( $T = 273.15$  K,  $p = 1013.25$  hPa).

$O_3$ ,  $SO_2$ ,  $NO$ ,  $NO_2$  instruments have a fairly constant signal response and were thus calibrated before and after the ETMEP-2 measurement campaign with external calibration gases. The factory calibration was used for the pressure, temperature and relative humidity sensors. The measurements were synchronized using their individual lag and response times. Please note that all mercury (TGM and GEM) concentrations are reported at standard temperature and pressure (STP;  $T = 273.15$  K,  $p = 1013.25$  hPa). At these standard conditions  $1 \text{ ng m}^{-3}$  corresponds to a mixing ratio of 112 ppqv (parts per quadrillion by volume).

### 3 Results

The first vertical profile was measured on 19 August 2013 from 11:15 to 12:15 UTC over the GMOS master site, Iskraba (Fig. 1). As Iskraba is located in mountainous terrain, the lowermost flight level was at 1000 m a.s.l. The measurements are summarized in Fig. 3. The squares represent the constant flight level measurement points (2 measurements at 2.5 min each). The stars represent the measurements while climbing between two flight levels (2.5 min average). The data represented by squares are thus more significant and the data illustrated by stars provide additional information of the vertical structure. Please note that the RH and the air temperature ( $T$ ) are plotted with high temporal resolution (1 s) in the rightmost panel. RH increases with increasing altitude and shows no step change to lower RH, which would identify the top of the PBL. Hence, the whole profile

in Fig. 3 was flown within the PBL. The measurements indicate a very constant mercury concentration without any vertical gradient for TGM and GEM. At  $1.44 \text{ ng m}^{-3}$  the whole column average TGM concentration was somewhat below the northern hemispheric background concentrations of  $1.5\text{--}1.7 \text{ ng m}^{-3}$  (Lindberg et al., 2007), but was comparable with the August 2013 monthly median of  $1.41 \text{ ng m}^{-3}$  at Mace Head, Ireland (Weigelt et al., 2015) and a median concentration of  $1.40 \text{ ng m}^{-3}$  of all vertical profiles over Tennessee, US, in 2012–2013 (Brooks et al., 2014). At  $1.38 \text{ ng m}^{-3}$  the column-averaged GEM concentration was only slightly lower than TGM, but this difference is smaller than the combined uncertainties of both instruments and thus insignificant. No ground-based reference data for the GMOS Iskraba site were available due to technical reasons. Besides mercury, neither  $CO$ , nor  $O_3$ ,  $NO$ , and  $NO_2$  mixing ratios indicate a significant vertical gradient. Only the  $SO_2$  mixing ratio increased from 1000 to 1500 m a.s.l. and remained constant at higher altitudes. In general the measurements thus showed that the air over Iskraba was well mixed within the PBL.

After the flight over Iskraba was completed, the second vertical profile was flown on the same day about 80 km northwest over the former mercury mining area Idrija. Until the 1990s, Idrija was the second largest mercury mine in operation worldwide (Grönlund et al., 2005). This profile was measured between 12:25 and 13:25 UTC (Fig. 4). Due to the mountainous terrain the seven horizontal flight legs were performed within the altitude range 1350 to 3150 m a.s.l.

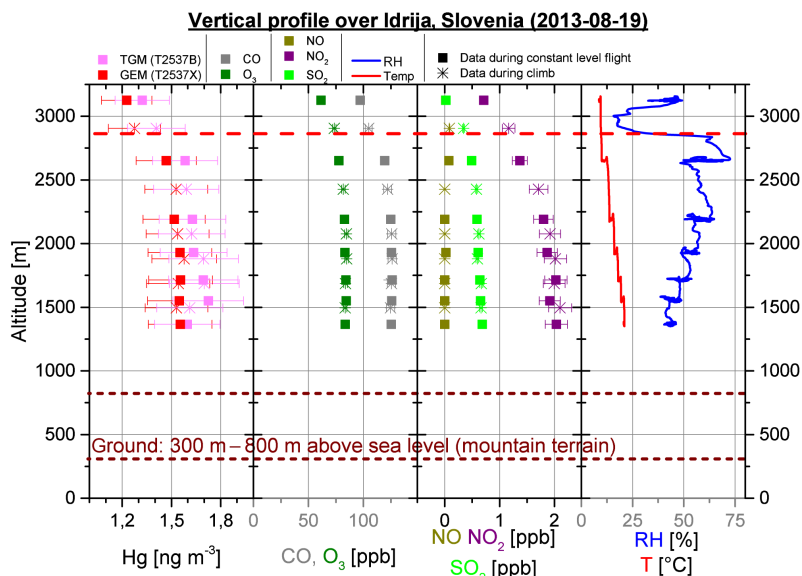


**Figure 4.** Same as Fig. 3, but for the former mercury mining area Idrija (45.000° N, 14.022° E, elevation: 330 m; mountain terrain up to 800 m). The profile was measured on 19 August 2013 from 14:30:00 to 15:20:00 (local time). The PBL top (red dashed line) was determined to be at 2850 to 2900 m a.s.l. TGM and GEM concentrations are given at standard temperature and pressure ( $T = 273.15$  K,  $p = 1013.25$  hPa).

Contrary to Iskraba, the uppermost flight leg over Idrija was flown above the PBL, in FT air. This is clearly indicated by a significantly reduced RH (the rightmost panel in Fig. 4). The boundary layer top was found at 2850 to 2900 m a.s.l.

Compared to Iskraba, the mercury concentration over Idrija was  $1.5$  to  $1.6$   $\text{ng m}^{-3}$  (GEM) and  $1.6$  to  $1.7$   $\text{ng m}^{-3}$  (TGM), about 10 to 15 % higher. The elevated mercury concentrations might be caused by increased emissions from the soil around Idrija, due to the legacy of the former mining activity. However, as over Iskraba, no vertical GEM or TGM concentration gradients were observed inside the PBL. It should be noted that above the PBL, GEM and TGM concentrations were found to be significantly lower (GEM:  $1.23$   $\text{ng m}^{-3}$ ; TGM:  $1.32$   $\text{ng m}^{-3}$ ;  $p = 0.999$ ). Ozone, CO, NO<sub>2</sub>, and SO<sub>2</sub> mixing ratios behave similarly, although NO<sub>2</sub> and SO<sub>2</sub> show a small gradient within the PBL, with slightly decreasing mixing ratios with increasing altitude. At 2700 m a.s.l. near the top of the PBL, all trace gas mixing ratios start to decrease and the mixing ratios at 3150 m a.s.l. in the FT are the lowest of the whole profile. O<sub>3</sub> and CO mixing ratios decrease by about 20 % when entering FT, NO<sub>2</sub> by about 60 % and SO<sub>2</sub> drops essentially to the detection limit. This step in mixing ratio at the PBL top indicates that FT air is separated from the PBL air due to slow air mass exchange. Nitrogen oxide (NO) shows no vertical gradient from inside the PBL to the FT. It should be noted the NO mixing ratios are close to the instrument's detection limit and might not be represented or have at least a large uncertainty. The stars at 2900 m a.s.l. represent a mixture of the PBL and FT air, explaining the concentrations found between the PBL

and FT air concentrations (e.g. GEM  $1.3$   $\text{ng m}^{-3}$  and TGM  $1.4$   $\text{ng m}^{-3}$ ).

On 21 August 2013, two vertical profiles were measured over central Germany in the Leipzig area (Fig. 1). The first profiling was carried out downwind of a coal-fired power plant and is the subject of another paper (Weigelt et al., 2016). Thereafter, the second profile was flown between 11:10 and 12:10 UTC over the city centre of Leipzig (population 500 000). The Leipzig profile was flown upwind of the power plant and was taken as a reference for the profile downwind of the power plant measurements. The profile is shown in Fig. 5. The lowermost flight level over Leipzig was 450 m above ground (600 m a.s.l.) and the highest one was 3020 m a.s.l.

From 21 to 23 August 2013, four additional CARIBIC flights were performed aboard a passenger aircraft (Lufthansa airbus A340-600) from Frankfurt, Germany to Caracas, Venezuela and Vancouver, Canada and back. Among other instruments (Brenninkmeijer et al., 2007), the CARIBIC system carries a Tekran 2537A mercury analyser, measuring TGM along the flight track with a temporal resolution of 600 s (Ebinghaus et al., 2007; Slemr et al., 2014, 2016). On 21 to 23 August 2013, a high pressure system dominated the weather over Germany and western Europe when the ETMEP-2 and the CARIBIC measurements were carried out. The wind direction in the free troposphere (3–10 km) was west to north-west and the forward and backward trajectory analysis showed that both the ETMEP-2 and CARIBIC aircraft sampled about the same air mass (see Fig. S1, Supplement). As will be shown below with the discussion of Fig. 5, the trace gases measured aboard

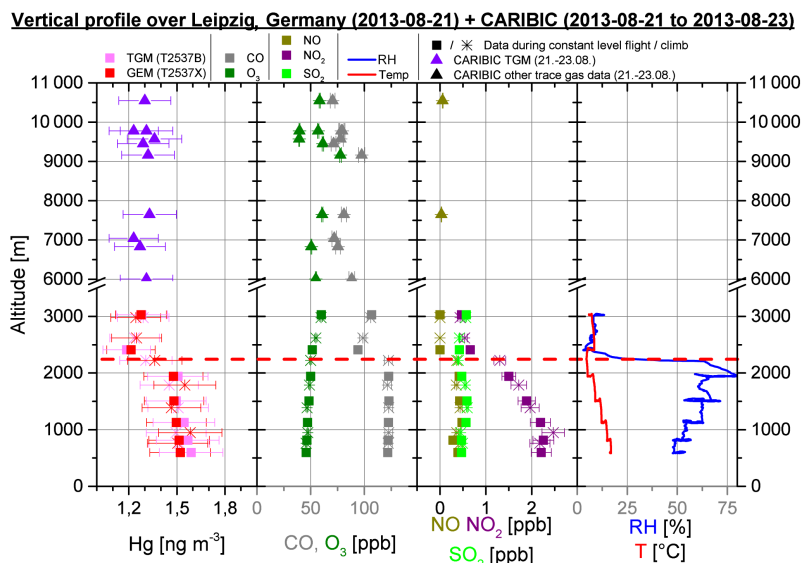


**Figure 5.** Vertical profile, measured within the ETMEP-2 campaign on 21 August 2013 from 13:15:00 to 14:07:30 (local time) over the city centre of Leipzig, Germany (51.353° N, 12.434° E, elevation: 125 m, flat terrain) and from 21 to 23 August 2013 over western Europe (east of 0° W; CARIBIC). While the ETMEP-2 data were averaged for 300 s (squares) and 150 s (stars), the CARIBIC data (triangles) represent 600 s averages. The plots have the same structure as Fig. 3. The PBL top (red dashed line) was determined to be at 2200 to 2250 m a.s.l. Please note that the y axis is broken between 3500 and 6000 m. TGM and GEM concentrations from ETMEP-2 and CARIBIC measurements are given at standard temperature and pressure ( $T = 273.15$  K,  $p = 1013.25$  hPa).

both aircraft match very well, which supports the notion that the same FT air mass was sampled during the CARIBIC and ETMEP-2 flights. This allows for supplementing and comparing the ETMEP-2 Leipzig TGM vertical profile with the independent CARIBIC measurements during ascent and descent from/to Frankfurt Airport, only some 350 km apart. For this extension only free-tropospheric CARIBIC measurements from 21 to 23 August 2013 east of 0° E are additionally plotted in Fig. 5, providing a vertical profile extending from 600 to 10 500 m a.s.l. Stratospheric CARIBIC measurements (with  $O_3 > 80$  ppb) are not shown.

The ETMEP-2-measured RH vertical profile identified the PBL top over the city centre of Leipzig at 2200 to 2250 m a.s.l. While the first five ETMEP-2 horizontal flight legs were flown inside the PBL, the last two legs were performed in FT air. Again, inside and above the PBL no vertical gradient was apparent for GEM, TGM,  $O_3$ , CO, NO, and  $SO_2$ , indicating well-mixed air masses. Only for  $NO_2$  a negative vertical gradient was found inside the PBL, but not above. Inside the PBL the average GEM and TGM concentrations were 1.50 and 1.55  $ng\ m^{-3}$ , which is in between the concentrations found inside the PBL over Iskraba and Idrija. The FT GEM and TGM concentrations over Leipzig were 1.2 to 1.3  $ng\ m^{-3}$ . Similar concentrations were also found in the FT air over Idrija (Fig. 4) and Waldhof (Fig. 6, flight leg five and six), as well as during the transfer flights Ronchi dei Legionari–Leipzig and Leipzig–Parma (not shown).

The CARIBIC and ETMEP-2 FT data match very well (Fig. 5). The average TGM concentration is 1.23  $ng\ m^{-3}$  for the ETMEP-2 and 1.30  $ng\ m^{-3}$  for the CARIBIC data set. This means that the measurements carried out in this study (August 2013) revealed no vertical TGM gradient in the entire FT over central Europe. Inside the PBL the GEM and TGM concentrations were found to be about 20 % higher. Furthermore the other trace gases measured on both aircraft match very well too. The difference was only 20 ppb or 20 % for CO, 0.2 ppb or < 1 % for  $O_3$ , and 0.05 ppb for NO (difference in % is not given because both values are close to zero). As indicated above, this agreement further supports the notion that the same FT air mass was sampled during the CARIBIC and ETMEP-2 flights. Consequently, the combined ETMEP-2 and CARIBIC data set provides, to the best of our knowledge, the first complete vertical mercury profiles from inside the PBL to the upper FT.

The last vertical profile was flown on 22 August 2013 over the GMOS master site in Waldhof (Fig. 6). Since this profile was measured in the late morning (08:15 to 09:15 UTC; 10:15 to 11:15 local time), the PBL was found to be rather shallow at 1750–1850 m a.s.l. when compared to the previous profiles. Thus only the first four flight legs were flown inside the PBL and the remaining three were above. As measured during all previous vertical profiles, a significant difference between PBL and FT air was again apparent for GEM and TGM concentrations, and CO, NO, and  $SO_2$  mixing ratios. The two lower FT flight legs indicated typical GEM and

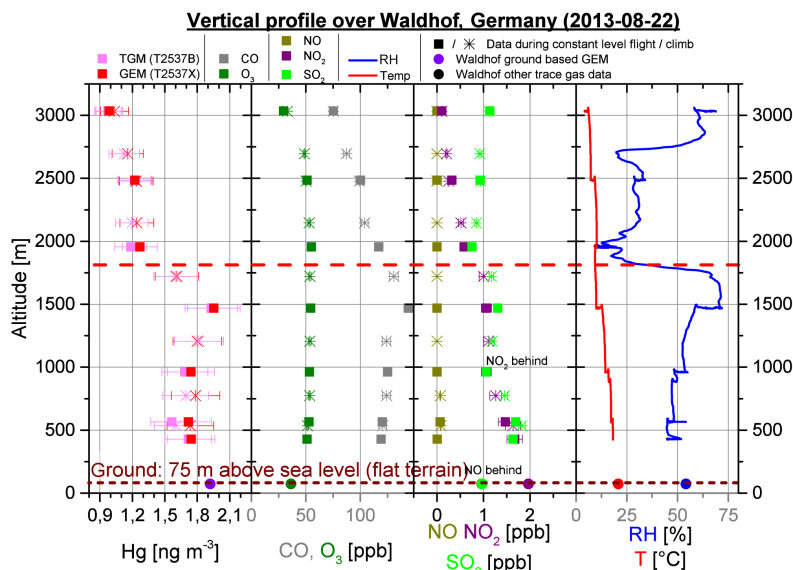


**Figure 6.** Same as Fig. 3, but over the GMOS master site Waldhof, Germany (52.801° N, 10.756° E, elevation: 75 m, flat terrain). The profile was measured on 22 August 2013 from 10:22:30 to 11:17:30 (local time). The PBL top (red dashed line) was determined to be at 1750 to 1850 m a.s.l. Additionally the data measured at the same time at the ground-based site Waldhof are plotted. TGM and GEM concentrations are given at standard temperature and pressure ( $T = 273.15$  K,  $p = 1013.25$  hPa).

TGM concentrations of  $1.27$  and  $1.19$   $\text{ng m}^{-3}$  (1950 m a.s.l.) and  $1.22$  and  $1.22$   $\text{ng m}^{-3}$  (2490 m a.s.l.) respectively. However, in the uppermost flight level at 3030 m a.s.l. GEM and TGM concentrations were  $0.99$  and  $0.98$   $\text{ng m}^{-3}$  respectively, i.e. about 25 % lower. Furthermore, in that layer not only the GEM and TGM concentrations, but also the CO and O<sub>3</sub> mixing ratios were about  $\sim 25$  % lower. At the same time RH was substantially higher at 66.6 % and SO<sub>2</sub> slightly higher at 1.1 ppb. Five-day backward trajectories (Fig. S2, Supplement) suggest that the air from this uppermost flight leg originated from the subtropical east Atlantic (about 30° N, 25° W). On the contrary, the air measured during all lower flight legs (in PBL and FT air) came from north Canada (north of 60° N, west of 50° W).

Inside the PBL, the GEM and TGM concentrations were at  $1.93$  and  $1.95$   $\text{ng m}^{-3}$  respectively, the highest in the uppermost flight leg (1470 m a.s.l.). Similarly, the CO mixing ratio was also elevated and the SO<sub>2</sub> raw signal indicated some short peaks to 1.5 ppb (not shown). The coincidence of elevated GEM and TGM concentrations with elevated CO and SO<sub>2</sub> mixing ratios was probably caused by a combustion plume. Below this plume a fairly constant profile was again measured for GEM ( $1.66$   $\text{ng m}^{-3}$ ), TGM ( $1.73$   $\text{ng m}^{-3}$ ), CO (121.4 ppb), O<sub>3</sub> (52.4 ppb), and NO (at detection limit). Only NO<sub>2</sub> and SO<sub>2</sub> mixing ratios increased towards the ground from 1.1 and 1.1 ppb, at 962 m a.s.l. to 1.7 and 1.6 ppb at 429 m a.s.l. respectively.

The GEM concentration measured by the speciation unit at the ground at the Waldhof site was somewhat elevated at  $1.92$   $\text{ng m}^{-3}$ . The Waldhof 3-year average (2009–2011)

GEM concentration is  $1.61$   $\text{ng m}^{-3}$  (Weigelt et al., 2013). At 2.0 ppb the ground-based NO<sub>2</sub> mixing ratio follows the increasing gradient toward the ground. On the contrary the Waldhof NO mixing ratio was significantly higher (1.0 ppb), and O<sub>3</sub> (36.4 ppb) and SO<sub>2</sub> (1.0 ppb) mixing ratios were somewhat lower than the airborne measurements. The measured air temperature and pressure, however, matched very well.

#### 4 Conclusions

In contrast to most of the previously reported vertical profiles, we always observed a significant difference between PBL and FT air (Fig. 7,  $p = 0.999$ ). While the FT GEM and TGM background concentrations over central Europe were  $\sim 1.3$   $\text{ng m}^{-3}$ , 10–30 % higher GEM and TGM concentrations were found in the PBL. The sharp gradient at the PBL top is probably caused by atmospheric dynamics. Mercury is emitted to the PBL by various sources (Pirrone et al., 2010; Song et al., 2015). The PBL is somewhat decoupled from the FT due to dynamic processes like friction and convection processes (Stull, 1988). Therefore, the exchange between PBL and the FT is inhibited, creating a gradient between the PBL and FT with higher concentrations in the PBL. The same applies for CO and SO<sub>2</sub> (Figs. 4–6) which are also emitted on the ground. Other dynamically caused mercury gradients can be found at the tropopause which inhibits exchange from the upper troposphere to the lower stratosphere (Slemr et al., 2009; Lyman and Jaffe, 2011), and at the intertropical convergence zone (Slemr et al., 1985; Temme et

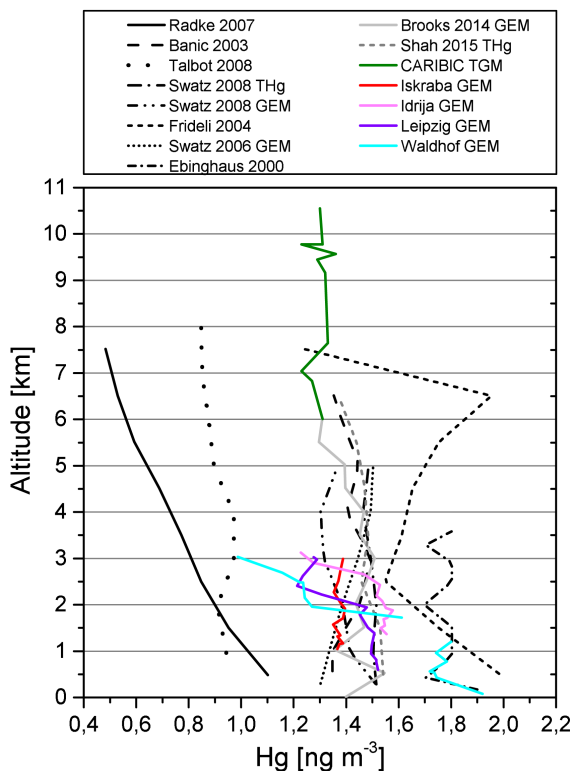


**Figure 7.** Comparison of known vertical gaseous mercury profiles (THg, TGM and GEM). Data plotted in black were taken from Swartzendruber et al. (2009). Data in grey represent the August measurement from Brooks et al. (2014) and the averaged data from Shah et al. (2016). Coloured data represent ETMEP-2 data (Figs. 3–6). The Waldhof 1.47 km flight leg average was removed from this plot, because it was probably measured inside a plume of polluted air (cf. discussion to Fig. 6).

al., 2003b), which inhibits transport from the northern to the southern hemisphere.

Besides the strong concentration gradient at the PBL top, at all sampling locations, neither in the boundary layer, nor in the free troposphere, a clear vertical gradient was apparent. This is in agreement with most of the vertical profiles obtained elsewhere (Swartzendruber et al., 2009; Brooks et al., 2014; Shah et al., 2016). Vertical profiles which have pronounced decreasing GEM concentrations with increasing altitude were reported by Radke et al. (2007) and Brooks et al. (2014), but only for the spring months of April, May, and June. These are the months with the strongest stratosphere to troposphere ozone flux in the northern hemisphere (Olsen et al., 2004) and the anomalous vertical profiles with strong vertical GEM gradients may be related to it. In the summer months GEM and TGM are homogeneously distributed inside the PBL and FT. The combination of ETMEP-2 measurements over Leipzig with CARIBIC measurements over western Europe (Fig. 5) gives a unique vertical profile from 0.5 km (lower PBL) to 10.5 km (upper FT). From above the

PBL to the FT top, the TGM background concentration is on average  $1.3 \text{ ng m}^{-3}$ .

Although the profile measurements were carried out within a short period, we believe that they are representative for summer conditions in central Europe. We measured similar concentrations at all flight levels of all measurement locations (except the above discussed PBL–FT difference) and they agree with the well-established northern hemispheric background concentration of  $1.5\text{--}1.7 \text{ ng m}^{-3}$  (Lindberg et al., 2007).

**The Supplement related to this article is available online at doi:10.5194/acp-16-4135-2016-supplement.**

*Acknowledgements.* Measurements were carried out as part of the European Tropospheric Mercury Experiment (ETMEP) within the Global Mercury Observation System project (GMOS; www.gmos.eu). GMOS is financially supported by the European Union within the seventh framework programme (FP-7, Project ENV.2010.4.1.3-2). Special thanks to Compagnia Generale Ripreseaeree (<http://www.terraitaly.it/>) in Parma, Italy and the pilots Oscar Gaibazzi and Dario Sassi for carrying out the measurement flights. Furthermore, we thank the whole IAGOS-CARIBIC team (www.caribic-atmospheric.com) for carrying out the measurement flights. Last but not least, we thank the German Federal Environmental Agency (Umweltbundesamt) and the Waldhof team for the ground-based measurements at the Waldhof site.

The article processing charges for this open-access publication were covered by a Research Centre of the Helmholtz Association.

Edited by: A. Dastoor

## References

- Ambrose, J. L., Gratz, L. E., Jaffe, D. A., Campos, T., Flocke, F. M., Knapp, D. J., Stechman, D. M., Stell, M., Weinheimer, A. J., Cantrell, C. A., and Mauldin, R. L.: Mercury emission ratios from coal-fired power plants in the southeastern United States during NOMADSS, *Environ. Sci. Technol.*, 49, 10389–10397, doi:10.1021/acs.est.5b01755, 2015.
- Banic, C. M., Beauchamp, S. T., Tordon, R. J., Schroeder, W. H., Steffen, A., Anlauf, K. A., and Wong, H. K. T.: Vertical distribution of gaseous elemental mercury in Canada, *J. Geophys. Res.*, 108, 4264, doi:10.1029/2002JD002116, 2003.
- Brenninkmeijer, C. A. M., Crutzen, P., Boumard, F., Dauer, T., Dix, B., Ebinghaus, R., Filippi, D., Fischer, H., Franke, H., Frieß, U., Heintzenberg, J., Helleis, F., Hermann, M., Kock, H. H., Koepfel, C., Lelieveld, J., Leuenberger, M., Martinsson, B. G., Miemczyk, S., Moret, H. P., Nguyen, H. N., Nyfeler, P., Oram, D., O’Sullivan, D., Penkett, S., Platt, U., Pupek, M., Ramonet, M., Randa, B., Reichelt, M., Rhee, T. S., Rohwer, J., Rosenfeld, K.,

- Scharffe, D., Schlager, H., Schumann, U., Slemr, F., Sprung, D., Stock, P., Thaler, R., Valentino, F., van Velthoven, P., Waibel, A., Wandel, A., Waschitschek, K., Wiedensohler, A., Xueref-Remy, I., Zahn, A., Zech, U., and Ziereis, H.: Civil Aircraft for the regular investigation of the atmosphere based on an instrumented container: The new CARIBIC system, *Atmos. Chem. Phys.*, 7, 4953–4976, doi:10.5194/acp-7-4953-2007, 2007.
- Brooks, S., Ren, X., Cohen, M., Luke, W. T., Kelley, P., Artz, R., Hynes, A., Landing, W., and Martos, B.: Airborne vertical profiling of mercury speciation near Tullahoma, TN, USA, *Atmosphere*, 5, 557–574, doi:10.3390/atmos5030557, 2014.
- Brosset, C.: The behavior of mercury in the physical environment, *Water Air Soil Pollut.*, 34, 145–166, 1987.
- Ebinghaus, R. and Slemr, F.: Aircraft measurements of atmospheric mercury over southern and eastern Germany, *Atmos. Environ.*, 34, 895–903, doi:10.1016/S1352-2310(99)00347-7, 2000.
- Ebinghaus, R., Jennings, S. G., Schroeder, W. H., Berg, T., Donaghy, T., Guentzel, J., Kenny, C., Kock, H. H., Kvietskus, K., Landing, W., Mühleck, T., Munthe, J., Prestbo, E. M., Schneeberger, D., Slemr, F., Sommar, J., Urba, A., Wallschläger, D., and Xiao, Z.: International field intercomparison measurements of atmospheric mercury species at Mace Head, Ireland, *Atmos. Environ.*, 33, 3063–3073, doi:10.1016/S1352-2310(98)00119-8, 1999.
- Ebinghaus, R., Slemr, F., Brenninkmeijer, C. A. M., van Velthoven, P., Zahn, A., Hermann, M., O’Sullivan, D. A., and Oram, D. E.: Emissions of gaseous mercury from biomass burning in South America in 2005 observed during CARIBIC flights, *Geophys. Res. Lett.*, 34, 1–5, doi:10.1029/2006GL028866, 2007.
- Fitzgerald, W. F., Engstrom, D. R., Mason, R. P., and Nater, E. A.: The case for atmospheric mercury contamination in remote areas, *Environ. Sci. Technol.*, 32, 1–7, doi:10.1021/es970284w, 1998.
- Friedli, H. R., Radke, L. F., Prescott, R., Li, P., Woo, J.-H., and Carmichael, G. R.: Mercury in the atmosphere around Japan, Korea, and China as observed during the 2001 ACE-Asia field campaign: Measurements, distributions, sources, and implications, *J. Geophys. Res.*, 109, D19S25, doi:10.1029/2003JD004244, 2004.
- Grönlund, R., Edner, H., Svanberg, S., Kotnik, J., and Horvat, M.: Mercury emissions from the Idrija mercury mine measured by differential absorption lidar techniques and a point monitoring absorption spectrometer, *Atmos. Environ.*, 39, 4067–4074, doi:10.1016/j.atmosenv.2005.03.027, 2005.
- Jaffe, D., Prestbo, E., Swartzendruber, P., Weiss-Penzias, P., Kato, S., Takami, A., Hatakeyama, S., and Kajii, Y.: Export of atmospheric mercury from Asia, *Atmos. Environ.*, 39, 3029–3038, doi:10.1016/j.atmosenv.2005.01.030, 2005.
- Klemp, D., Mannschreck, K., Pätz, H. W., Habram, M., Matuska, P., and Slemr, F.: Determination of anthropogenic emission ratios in the Augsburg area from concentration ratios: Results from long-term measurements, *Atmos. Environ.*, 36, 61–80, doi:10.1016/S1352-2310(02)00210-8, 2002.
- Kvietskus, K.: Investigation of the gaseous and particulate mercury concentrations along horizontal and vertical profiles in the lower troposphere, in: Proceedings of the 10th World Clean Air Congress, Espoo, Finland, 28 May–2 June 1995: Atmospheric pollution, edited by: Anttala, P., Kämäri, J., and Jolvanen, M., 284–287, Finnish Air Pollution Prevention Society, Helsinki, 1995.
- Lindberg, S., Bullock, R., Ebinghaus, R., Engstrom, D., Feng, X., Fitzgerald, W., Pirrone, N., Prestbo, E., and Seigneur, C.: A synthesis of progress and uncertainties in attributing the sources of mercury in deposition, *AMBIO*, 36, 19–33, doi:10.1579/0044-7447(2007)36[19:ASOPAU]2.0.CO;2, 2007.
- Lyman, S. N. and Jaffe, D. A.: Formation and fate of oxidized mercury in the upper troposphere and lower stratosphere, *Nat. Geosci.*, 5, 114–117, doi:10.1038/ngeo1353, 2011.
- Olsen, M. A., Schoeberl, M. R., and Douglass, A. R.: Stratosphere-troposphere exchange of mass and ozone, *J. Geophys. Res.*, 109, D24114, doi:10.1029/2004JD005186, 2004.
- Parrish, D. D., Trainer, M., Buhr, M. P., Watkins, B. A., and Fehsenfeld, F. C.: Carbon monoxide concentrations and their relation to concentrations of total reactive oxidized nitrogen at two rural US sites, *J. Geophys. Res.*, 96, 9309–9320, doi:10.1029/91JD00047, 1991.
- Pirrone, N., Cinnirella, S., Feng, X., Finkelman, R. B., Friedli, H. R., Leaner, J., Mason, R., Mukherjee, A. B., Stracher, G. B., Streets, D. G., and Telmer, K.: Global mercury emissions to the atmosphere from anthropogenic and natural sources, *Atmos. Chem. Phys.*, 10, 5951–5964, doi:10.5194/acp-10-5951-2010, 2010.
- Radke, L. F., Friedli, H. R., and Heikes, B. G.: Atmospheric mercury over the NE Pacific during spring 2002: Gradients, residence time, upper troposphere lower stratosphere loss, and long-range transport, *J. Geophys. Res.*, 112, 1–17, doi:10.1029/2005JD005828, 2007.
- Scheele, M. P., Siegmund, P. C., and Van Velthoven, P. F. J.: Sensitivity of trajectories to data resolution and its dependence on the starting point: In or outside a tropopause fold, *Meteorol. Apps*, 3, 267–273, doi:10.1002/met.5060030308, 1996.
- Selin, N. E.: Global biogeochemical cycling of mercury: A review, *Annu. Rev. Environ. Resour.*, 34, 43–63, doi:10.1146/annurev.enviro.051308.084314, 2009.
- Shah, V., Jaeglé, L., Gratz, L. E., Ambrose, J. L., Jaffe, D. A., Selin, N. E., Song, S., Campos, T. L., Flocke, F. M., Reeves, M., Stechman, D., Stell, M., Festa, J., Stutz, J., Weinheimer, A. J., Knapp, D. J., Montzka, D. D., Tyndall, G. S., Apel, E. C., Hornbrook, R. S., Hills, A. J., Riemer, D. D., Blake, N. J., Cantrell, C. A., and Mauldin III, R. L.: Origin of oxidized mercury in the summertime free troposphere over the southeastern US, *Atmos. Chem. Phys.*, 16, 1511–1530, doi:10.5194/acp-16-1511-2016, 2016.
- Slemr, F., Schuster, G., and Seiler, W.: Distribution, speciation, and budget of atmospheric mercury, *J. Atmos. Chem.*, 3, 407–434, doi:10.1007/BF00053870, 1985.
- Slemr, F., Ebinghaus, R., Brenninkmeijer, C. A. M., Hermann, M., Kock, H. H., Martinsson, B. G., Schuck, T., Sprung, D., van Velthoven, P., Zahn, A., and Ziereis, H.: Gaseous mercury distribution in the upper troposphere and lower stratosphere observed onboard the CARIBIC passenger aircraft, *Atmos. Chem. Phys.*, 9, 1957–1969, doi:10.5194/acp-9-1957-2009, 2009.
- Slemr, F., Weigelt, A., Ebinghaus, R., Brenninkmeijer, C., Baker, A., Schuck, T., Rauthe-Schöch, A., Riede, H., Leedham, E., Hermann, M., van Velthoven, P., Oram, D., O’Sullivan, D., Dyroff, C., Zahn, A., and Ziereis, H.: Mercury plumes in the global upper troposphere observed during flights with the CARIBIC observatory from May 2005 until June 2013, *Atmosphere*, 5(2), 342–369, doi:10.3390/atmos5020342, 2014.

- Slemr, F., Weigelt, A., Ebinghaus, R., Kock, H. H., Böde-wadt, J., Brenninkmeijer, C. A. M., Rauthe-Schöch, A., Weber, S., Hermann, M., Zahn, A., and Martinsson, B.: Atmospheric mercury measurements onboard the CARIBIC passenger aircraft, *Atmos. Meas. Tech. Discuss.*, doi:10.5194/amt-2015-376, in review, 2016.
- Song, S., Selin, N. E., Soerensen, A. L., Angot, H., Artz, R., Brooks, S., Brunke, E.-G., Conley, G., Dommergue, A., Ebinghaus, R., Holsen, T. M., Jaffe, D. A., Kang, S., Kelley, P., Luke, W. T., Magand, O., Marumoto, K., Pfaffhuber, K. A., Ren, X., Sheu, G.-R., Slemr, F., Warneke, T., Weigelt, A., Weiss-Penzias, P., Wip, D. C., and Zhang, Q.: Top-down constraints on atmospheric mercury emissions and implications for global biogeochemical cycling, *Atmos. Chem. Phys.*, 15, 7103–7125, doi:10.5194/acp-15-7103-2015, 2015.
- Spencer, R. W. and Braswell, W. D.: How dry is the tropical free troposphere? Implications for global warming theory, *B. Am. Meteorol. Soc.*, 78, 1097–1106, doi:10.1175/1520-0477(1997)078<1097:HDITTF>2.0.CO;2, 1996.
- Stull, R. B.: *An Introduction to Boundary Layer Meteorology*, Atmospheric Sciences Library 13, Kluwer Academic Publishers, Dordrecht, doi:10.1007/978-94-009-3027-8, 1988.
- Swartzendruber, P. C., Jaffe, D. A., Prestbo, E. M., Weiss-Penzias, P., Selin, N. E., Park, R., Jacob, D. J., Strode, S., and Jaeglé, L.: Observations of reactive gaseous mercury in the free troposphere at the Mount Bachelor Observatory, *J. Geophys. Res.-Atmos.*, 111, D24301, doi:10.1029/2006JD007415, 2006.
- Swartzendruber, P. C., Chand, D., Jaffe, D. A., Smith, J., Reidmiller, D., Gratz, L., Keeler, J., Strode, S., Jaeglé, L., and Talbot, R.: Vertical distribution of mercury, CO, ozone, and aerosol scattering coefficient in the Pacific Northwest during the spring 2006 INTEX-B campaign, *J. Geophys. Res.-Atmos.*, 113, D10305, doi:10.1029/2007JD009579, 2008.
- Swartzendruber, P. C., Jaffe, D. A., and Finley, B.: Development and first results of an aircraft-based, high time resolution technique for gaseous elemental and reactive (oxidized) gaseous mercury, *Environ. Sci. Technol.*, 43, 7484–7489, doi:10.1021/es901390t, 2009.
- Talbot, R., Mao, H., Scheuer, E., Dibb, J., and Avery, M.: Total depletion of Hg<sup>0</sup> in the upper troposphere-lower stratosphere, *Geophys. Res. Lett.*, 34, L23804, doi:10.1029/2007GL031366, 2007.
- Talbot, R., Mao, H., Scheuer, E., Dibb, J., Avery, M., Browell, E., Sachse, G., Vay, S., Blake, D., Huey, G., and Fuelberg, H.: Factors influencing the large-scale distribution of Hg<sup>0</sup> in the Mexico City area and over the North Pacific, *Atmos. Chem. Phys.*, 8, 2103–2114, doi:10.5194/acp-8-2103-2008, 2008.
- Temme, C., Einax, J. W., Ebinghaus, R., and Schroeder, W. H.: Measurements of atmospheric mercury species at a coastal site in the Antarctic and over the South Atlantic Ocean during polar summer, *Environ. Sci. Technol.*, 37, 22–31, doi:10.1021/es025884w, 2003a.
- Temme, C., Slemr, F., Ebinghaus, R., and Einax, J. W.: Distribution of mercury over the Atlantic Ocean in 1996 and 1999–2001, *Atmos. Environ.*, 37, 1889–1897, doi:10.1016/S1352-2310(03)00069-4, 2003b.
- Weigelt, A., Temme, C., Bieber, E., Schwerin, A., Schuetze, M., Ebinghaus, R., and Kock, H. H.: Measurements of atmospheric mercury species at a German rural background site from 2009 to 2011 – methods and results, *Environ. Chem.*, 10, 102–110, doi:10.1071/EN12107, 2013.
- Weigelt, A., Ebinghaus, R., Manning, A. J., Derwent, R. G., Simmonds, P. G., Spain, T. G., Jennings, S. G., and Slemr, F.: Analysis and interpretation of 18 years of mercury observations since 1996 at Mace Head, Ireland, *Atmos. Environ.*, 100, 85–93, doi:10.1016/j.atmosenv.2014.10.050, 2015.
- Weigelt, A., Slemr, F., Ebinghaus, R., Pirrone, N., Bieser, J., Böde-wadt, J., Esposito, G., and van Velthoven, P. F. J.: Airborne measurements of mercury emissions from a modern coal fired power plant in central Europe, in preparation, 2016.
- Zahn, A. and Brenninkmeijer, C. A.: New directions: A chemical tropopause defined, *Atmos. Environ.*, 37, 439–440, doi:10.1016/S1352-2310(02)00901-9, 2003.